A NEW DOUBLY SALIENT PERMANENT MAGNET MOTOR FOR ADJUSTABLE SPEED DRIVES

YUEFENG LIAO and T. A. LIPO

Department of Electrical and Computer Engineering
University of Wisconsin-Madison
1415 Johnson Drive
Madison, WI 53706, USA

ABSTRACT: A new type of doubly salient motor is presented in this paper in which the field excitation is provided by permanent magnets. This doubly salient Permanent Magnet (DSPM) motor is shown to be kindred to square waveform permanet magnet brushless dc (PM-BLDC) motors in principle. However, they are different from the latter in that they are capable of a considerable constant power range when properly designed. Finite Element Analysis and Transient Simulation studies are utilized to investigate the characteristics of this new type of PM motor. A prototype DSPM motor is designed and comparison is made between this new type of motor and other types of motor on the basis of performance of the entire drive. By fully exploiting the merits of modern high energy PM material and the doubly salient structure, the DSPM motor can offer higher performance expectation over many existing motors in terms of efficiency, torque density, torque-to-current ratio, torque-to-inertia ratio etc. with a relatively simple structure which is amenable to automatic manufacture.

1. INTRODUCTION

Variable Reluctance Motors (VRMs) have been the focus of extensive research efforts during the past decade and its torque production, design and control characteristics have been well explored[1-3]. In particular, its inherent fault-tolerant feature, among other merits claimed by its proponents, has been well demonstrated so that the variable reluctance motor is becoming a prime candidate for reliability-premium applications[4].

The VRM is very unique as viewed from the point of view of energy conversion. However, its uniqueness also gives rise to a number of problems in terms of torque production. Firstly, because the motor operates in a mode in which the field energy needs to be extracted repeatedly from the machine when the active phase reaches a maximum inductance position, the problem of current commutation associated with the large turn-off inductance greatly decreases the torque production capability of the VRM fed by a non-ideal power converter with finite KVA. As a result, both the machine and the power converter are usually highly stressed from the point of view of voltage and current. Also, the airgap of the VRM must be substantially reduced compared to other competing machines to push the machine into the highly saturated region, which adversely offsets the low cost advantage of the VRM in addition to causing noise and torque pulsation. Finally, the variable reluctance action makes possible the use of only one of the two possible torque producing zones. That is, motoring torque can be produced only when the rotor is entering the region occupied by a given phase, i.e. when the inductance is decrease. Only braking torque can be produced if the phase is energized while the pole is leaving the aligned, maximum inductance position. The utilization of the active materials is consequently very poor in the VRM. These problems make the torque production of the VRM much less effective that the Permanent Magnet brushless DC (PM-BLDC) motor.

This paper presents a new type of doubly salient motor in which the field excitation is supplied by permanent magnet built inside the motor. This new type of PM motor is realized by appropriately placing permanent magnet in the doubly salient structure of VRM's, thereby forming what can be termed a *doubly salient permanent magnet* (DSPM) motor. It should be noted that the DSPM motor described here is different from the hybrid PM stepping motor which is inherently a reluctance machine.[5] The PM is used in the hybrid PM stepping motor

Request reprints from T. A. Lipo. Manuscript received in final form January 4, 1993.

0731-356X/94 $10.00 + .00

to improve the dynamics and to produce holding torque, having no contribution to the average torque produced. The DSPM motor also distinguishes itself from the singly salient PM motor which is a straightforward extension of the VRM obtained by replacing the rotor with magnet poles[6]. Simple as it is, the singly salient PM motor is usually characterized by low airgap flux density and poor utilization of the PM material, which adversely affect its torque density and efficiency.

The use of separate field excitation, either with electrical means or via permanent magnets, in a doubly salient machine has a long history in industrial applications in the guise of homopolar inductor machines, as can be found in the field of high speed, high frequency alternators[7-8]. Such homopolar inductor generators can be classified into two categories: (i) doubly salient machines with concentrated, short-pitched stator windings and (ii) singly salient machines with conventional, sinusoidally distributed stator windings. The latter has largely evolved into the well-known Lundell machine[9], while the former has been less well reported although frequently used as a high speed alternator[10]. Unlike the VRM, the doubly salient structure of a homopolar inductor machine serves mainly as flux guide, and the torque produced is dominated by reaction torque instead of by reluctance torque. Compared to synchronous machines, the homopolar inductor machine incurs a weight penalty due to the fact that the flux linking the armature is pulsating rather than alternating and also because of the need for additional space to accommodate the coaxial field winding and the returning flux paths[8]. Several attempts have been made to overcome this drawback, with the most notable being the Flux-Switch machine presented by Rauch and Johnson in 1955 as a high power density, high frequency single phase alternator[11]. A patent was filed by Zimmerman in 1956 based on the same principle, with the addition of a combined electrical and PM field excitation[12].

Recently, Philips proposed the use of an additional full-pitched winding in the VRM as a field winding in an attempt to improve its torque production, based on the concept of Pre-magnetization[13]. Philips' work is an improvement over an earlier implementation of the same concept by Torok which evolved into a family of multiphase Electrical Reluctance Machines[14]. All of these machines can be viewed as field-assisted variable reluctance machines, with energy converted through the variable reluctance action as well as the interaction between armature current and field flux. Philips' proposal does improve on the energy ratio of the VRM. However, both Philips and Torok failed to recognize the uniqueness brought about by the use of PM excitation. As a result, torque production in this type of reluctance machine when used as a motor is very complicated and highly nonlinear.

It is the objective of the work as described here to exploit the torque production capability of the doubly salient machine by introducing permanent magnet excitation to advantage in such machines, thus eliminating all the above mentioned deficiencies of the VRM. Specifically, the use of modern high energy PM material completely eliminates the excitation penalty suffered by the VRM. Thus the power rating of the converter as well as the motor can be reduced considerably as compared to a conventional VRM. In addition, the existence of the magnet alters the electromagnetic structure of the motor, realizing a smaller inductance at the aligned position. This feature not only greatly decreases the commutation interval of the working current, but also makes it possible to reverse the current at the aligned position thereby making use of another torque producing zone which greatly increases the torque producing capability of the motor. This newly conceived DSPM motor can take on a homopolar, rotary magnet and stationary magnet structures[15]. This paper will focus on the DSPM motor with rotary PM, while a stationary magnet version of the DSPM motor will be described in a future paper[16].

2. BASIC PRINCIPLES OF OPERATION AND CONTROL

Figure 1 shows the cross-section of a 3-phase, 6/4-pole rotary magnet DSPM motor. This 3-phase, 6/4-pole configuration is the most simple pattern for motoring operation with satisfactory starting performance. For low speed and high torque applications, the machine can be constructed in repetitive fashion. However, 2-phase or even single phase schemes can be conceived for use as a generator only.

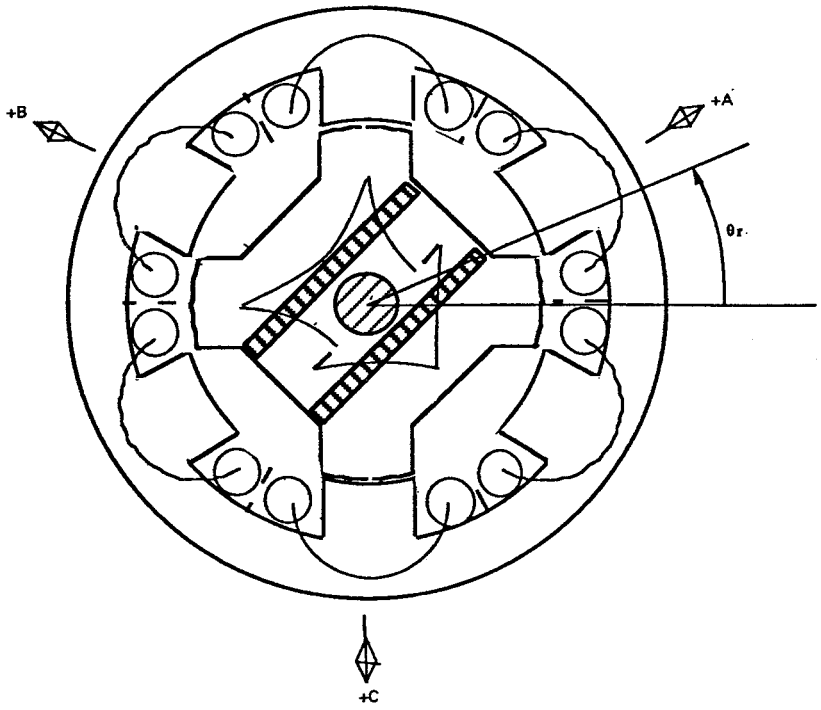

Fig. 1 Schematic of the DSPM Machine

The stator of the DSPM is identical to that of the 3-phase variable reluctance machine. The rotor structure is also similar to that of the VRM except that two pieces of PM are buried inside the rotor and therefore introduced into the main flux path of the stator windings. High performance PM material with linear demagnetizing characteristic is used to sustain the magnetization and demagnetization of the armature reaction, thus keep a constant flux level. The stator pole arc is set to be p/6 and the rotor pole arc to be slightly greater than the stator pole arc to allow for current reversal. As a result, the airgap reluctance, which forms the major part of the reluctance for the PM excitation, is invariant with the rotor position. A linear variation of the PM flux linkage and thus a trapezoidal back EMF is induced in the stator winding at no-load. When the machine is loaded, the bulk of the armature reaction flux is forced to circulate through another overlapped pole pair because the existence of the PM constitutes a high reluctance path for the flux. As a result, the active stator phase winding will possess small inductances at both aligned and unaligned positions, and the maximum inductance appears when the poles are half overlapped, with the value greatly reduced due to the effect of local saturation.

As a first approximation, the variations of the winding inductance and the PM induced flux linkage of an active stator phase winding are assumed to be piece-wise linear and spatially dependent only, as shown in Fig. 2. The terminal voltage equation for an active stator phase winding is

$$v = Ri + e \approx e = \frac{d\psi}{dt} \tag{1}$$

The flux linkage ψ is composed of the PM induced flux linkage ψ_m and the armature reaction flux linkage (Li):

$$\psi = Li + \psi_m \tag{2}$$

Therefore,

$$e = \frac{d\psi}{dt} = L\frac{di}{dt} + i\frac{dL}{dt} + \frac{d\psi_m}{dt}$$

$$= L\frac{di}{dt} + e_r + e_m \tag{3}$$

This result suggests the simple equivalent circuit of Fig. 3.

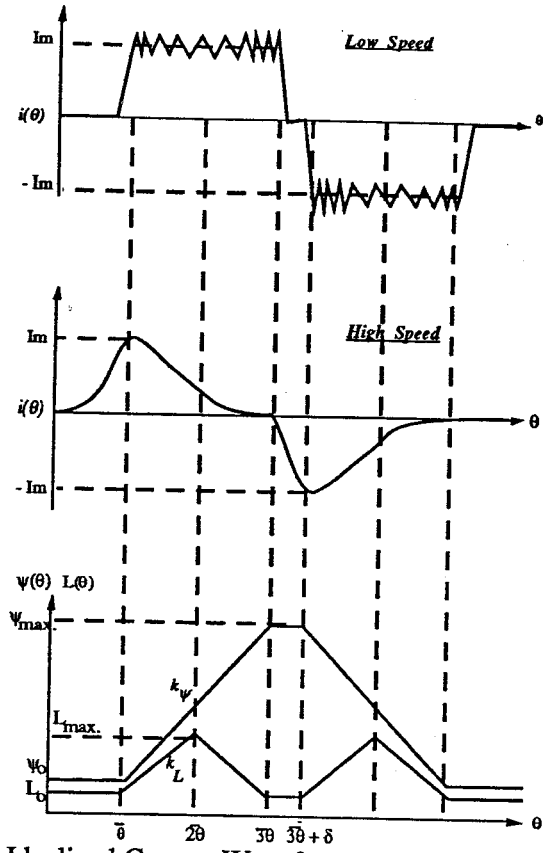

Fig. 2 Idealized Current Waveforms of the DSPM Motor.

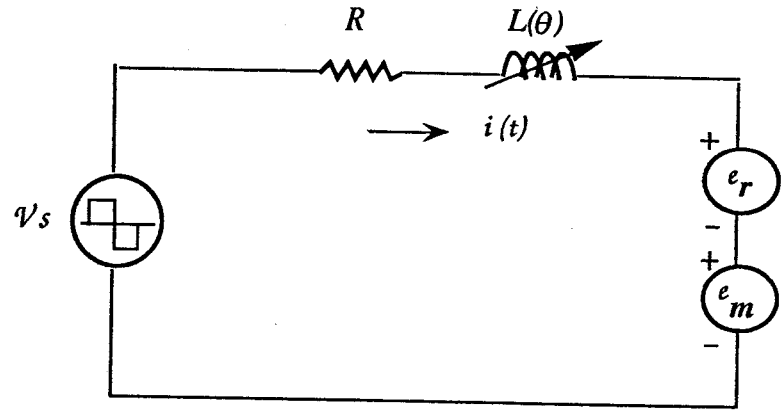

Fig. 3 Equivalent Circuit of the DSPM Motor.

The electrical power entering into the winding is, neglecting ohmic and iron losses,

$$P_e = e\,i$$

$$= iL\frac{di}{dt} + i\,2\frac{dL}{dt} + i\,\frac{d\psi_m}{dt}$$

$$= \frac{d}{dt}[\frac{1}{2}Li^2] + \{\frac{1}{2}i^2\frac{\partial L}{\partial \theta_r} + i\frac{\partial \psi_m}{\partial \theta_r}\}\omega_r \quad (4)$$

Power balance gives

$$P_e = \frac{d}{dt}W_{fs} + T\omega_r \quad (5)$$

Hence we have

$$T = \frac{1}{2}i^2\frac{\partial L}{\partial \theta_r} + i\frac{\partial \psi_m}{\partial \theta_r}$$

$$= T_r + T_m \quad (6)$$

and

$$W_{fs} = \frac{1}{2}Li^2 \quad (7)$$

Careful examination of Eqn.(6) and Eqn.(7) reveals the following features of the DSPM motor:

(i) The armature reaction field energy W_{fs}, which is to be recovered during current commutation, is very small because of the small value of the stator inductance. Therefore, the energy conversion ratio, or equivalently the power factor, is almost unity;

(ii) Because of the triangle-shaped variation of the stator winding inductance, the reluctance torque T_r will be of zero average value if the current is kept constant during one stroke. However, the net reluctance torque will be non-zero if the current is varying;

(iii) The reaction torque T_m, which is the dominant torque component, can be produced by applying either a positive current to a phase winding when its flux linkage is increasing (or $e_m > 0$) or a negative current when the flux linkage is decreasing (or $e_m < 0$).

It is clear that at low speed, the DSPM motor is, in principle, similar to the PM-BLDC motor with 240° conducting, quasi-square current waveform. The only difference is that the two 120° conducting current blocks are drawn closer in the case of the DSPM motor. It should be realized that enough interval between the two current blocks must be provided in the design of the DSPM motor to ensure current reversal. At high speed, the current cannot be maintained constant due to the excessive PM induced back EMF. The current peaks in the first half stroke where the inductance is increasing and drops rapidly in the second half stroke where the inductance is decreasing. The uneven distribution of the phase current gives rise to a considerable amount of reluctance torque which contributes to the constant power capability of the DSPM motor. This feature distinguishes the DSPM motor from the PM-BLDC motor.

Control of the DSPM motor is similar to that of the PM BLDC motor. Four quadrant operation is easily achieved by changing the sequence of conduction and the direction of current. Below the base speed, current regulation is used to achieve smooth torque production. Above the base speed, the motor becomes voltage fed, similar to the single pulse operation of the VRM. Angle control is utilized in order to realize a constant power range above base speed.

3. DESIGN AND NONLINEAR ANALYSIS

3.1. Design of the Prototype DSPM Motor

A prototype DSPM motor has been designed to support the theory outlined above. This prototype machine was chosen intentionally to have the same frame size as those

selected by T.J.E. Miller for a meaningful comparison[17]. As such, the design is not optimized. The stator copper losses in all these motors are also kept almost the same to place all motors under the same cooling conditions. For the purpose of a fair comparison, the same permanent magnet material (NdIGT-30H) is used in the design of the DSPM motor. The laminated steel is assumed to be of M19 AISI grade. Details of the design are included in Appendix.

3.2 Finite Element Analysis

Finite Element Analysis (FEA) has been employed as a tool for accurate steady state modelling and performance analysis of the DSPM machines, accounting for magnetic saturation, fringing and demagnetization. Finite element method was applied to the calculation of the two dimensional magnetic field distribution in the cross section of the DSPM machines. The field solution data was then processed to obtain dynamic and steady state characteristics of the motor.

The prototype DSPM motor was extensively analyzed using MSC/EMAS, a general purpose field analysis package. Figure 4 shows the finite element mesh. The flux contour plots for two time instants are shown in Fig. 5. It can be observed that the flux is mainly concentrated at the overlapped pole area. Figure 6 shows flux linkage vs. current curves of a specific stator winding computed at different rotor positions for the prototype DSPM motor. It can be seen that the armature reaction flux at full load condition is small, although appreciable. Also it is clear that the variations of flux linkage with respect to current at various rotor positions are almost linear up to 1.5 times rated current. This result suggests that the effects of the PM flux linkage can be separated from the armature reaction flux linkage which can be expressed as product of the stator current and a spatially dependent stator winding inductance.

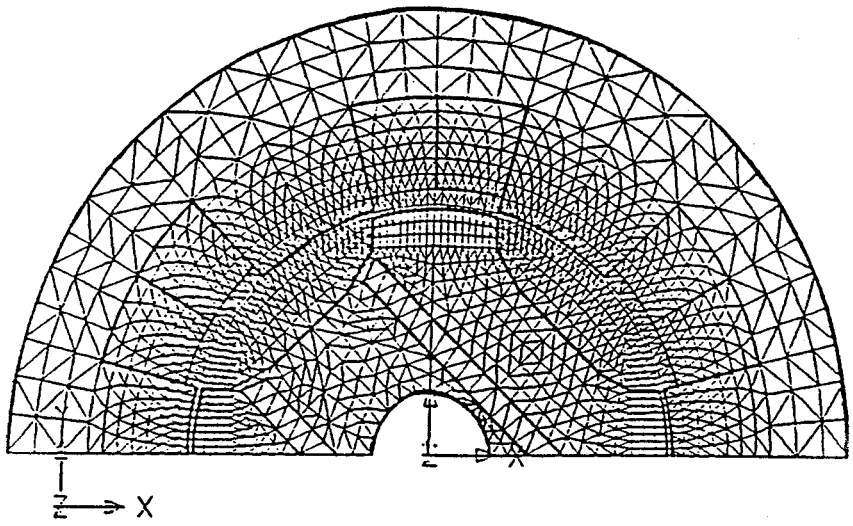

Fig. 4 Finite Element Mesh for the Prototype DSPM Motor.

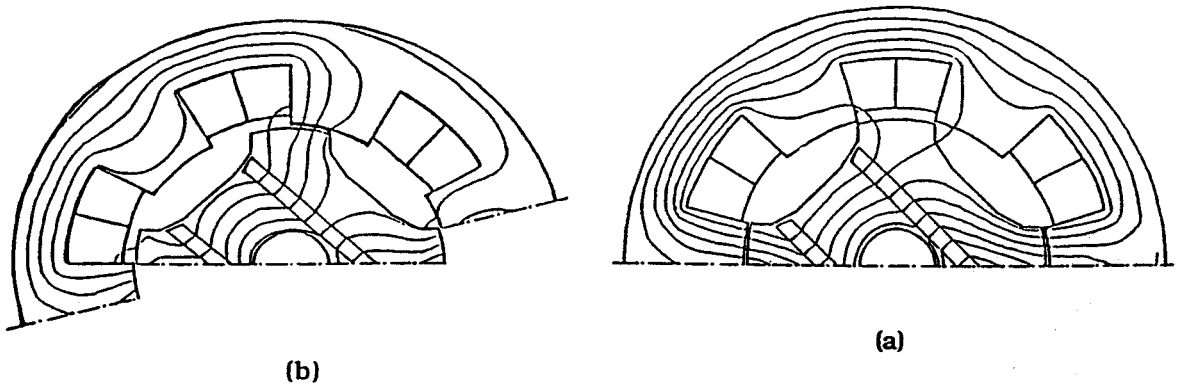

Fig. 5 Flux Contours for the Prototype DSPM Motor

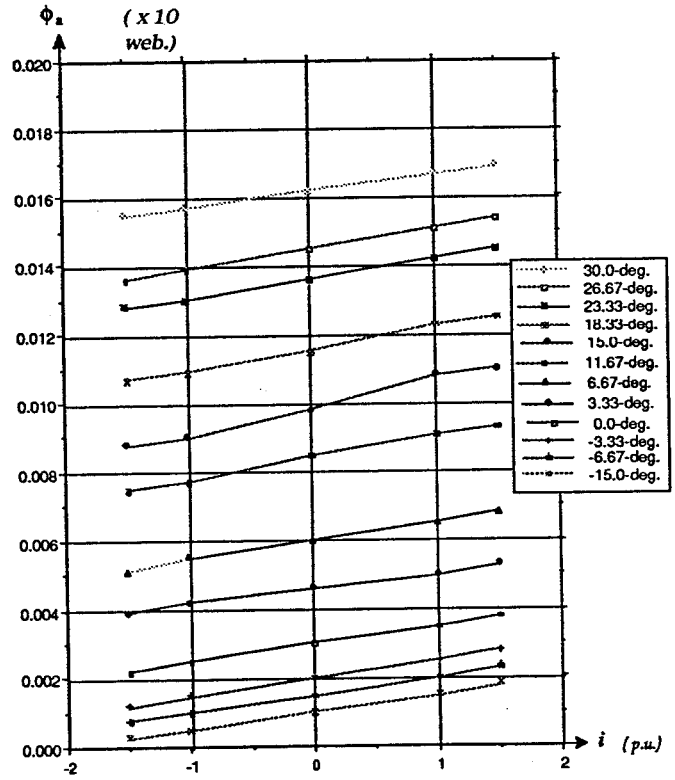

Fig. 6 Stator Flux Linkage vs. Current Obtained by FEA

3.3 Dynamic Simulation

The DSPM motor drive is shown schematically in Fig. 7. The model consists of an ideal DC voltage bus, an ideal inverter giving a vector of terminal voltages to the the stator windings of the motor according to the control scheme adopted, and a dynamic model of the DSPM motor. The dynamic model of the DSPM motor is derived in the stationary reference

frame in phase quantities, with special consideration given to the PM. The voltage and flux equations describing the motor are, in matrix forms, as follows,

$$\underline{V} = \underline{R}\,\underline{I} + \frac{d\underline{\Lambda}}{dt} = \underline{R}\,\underline{I} + \underline{E} \tag{8.a}$$

where

$$\underline{V} = \begin{pmatrix} v_1 \\ v_2 \\ v_3 \end{pmatrix}, \quad \underline{I} = \begin{pmatrix} i_1 \\ i_2 \\ i_3 \end{pmatrix}, \quad \underline{E} = \begin{pmatrix} e_1 \\ e_2 \\ e_3 \end{pmatrix}$$

and

$$\underline{\Lambda} = \underline{L}\,\underline{I} + \underline{\Lambda}_m \tag{8.b}$$

with

$$\underline{L} = \begin{pmatrix} L_{1s} & L_{12} & L_{13} \\ L_{21} & L_{2s} & L_{23} \\ L_{31} & L_{32} & L_{3s} \end{pmatrix}, \underline{R} = \begin{pmatrix} \mathcal{R}_1 & 0 & 0 \\ 0 & \mathcal{R}_2 & 0 \\ 0 & 0 & \mathcal{R}_3 \end{pmatrix}, \quad \underline{\Lambda}_m = \begin{pmatrix} \lambda_{m1} \\ \lambda_{m2} \\ \lambda_{m3} \end{pmatrix}$$

$\underline{L}$ and $\underline{\Lambda}_m$ are assumed to be spatially dependent only, invariant of the stator current. Note that in contrast to the variable reluctance machine mutual inductances appear on the off diagonally of $\underline{L}$.

By the co-energy method, the equation for the torque can be written as

$$T_e = \frac{\partial W'}{\partial \theta_r} = \frac{\partial}{\partial \theta_r}\left[\frac{1}{2}\underline{I}^T \underline{L}\,\underline{I} + \underline{\Lambda}_m{}^T \underline{I}\right]$$

$$= \frac{1}{2}\underline{I}^T\left(\frac{\partial}{\partial \theta_r}\underline{L}\right)\underline{I} + \left(\frac{\partial}{\partial \theta_r}\underline{\Lambda}_m\right)^T \underline{I} \tag{9}$$

The first term in Eqn. (9) represents the reluctance torque due to variation of the inductances, and the second term is the reaction torque due to interaction between the winding current and the PM flux.

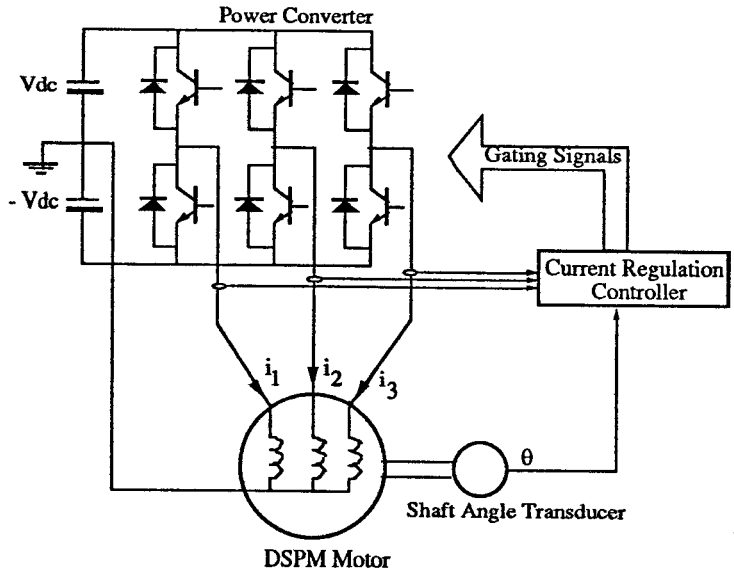

Fig. 7 DSPM Motor Drive Used for Modelling

Equation (8) can be expressed explicitly in terms of either flux linkage or current to be solved by numerical integration. Note that the inductance matrix and PM flux linkages are all position-dependant variables given by FEA. The evaluation of torque as per Eqn. (8) needs also the derivatives of the inductance matrix and PM flux linkages. The functional evaluation of the inductance matrix and PM flux linkages can be looked up during the simulation

through spline-interpolation, while the derivatives can be evaluated through numerical differentiation.

The waveforms of applied voltage and current of a stator phase winding (v_a, i_a) of the prototype DSPM motor and the torque produced by one phase (T_{ea}) as well as the total torque produced (T_e) obtained by dynamic simulation for speeds below and above the base speed are shown in Figs. 8-9. The phase current is kept constant by chopping at low speed. The reluctance torque, as a result, causes a ramp on the top of the torque profile. The build-up and decay of phase currents, especially during the commutating period, are attributable to the peaky torque ripples. At high speed, the active phase winding is turned on at an advanced angle to bring the current to a permissible peak value before the pole pair begins to overlap. The current then begins to collapse, followed by a successful current reversal at the aligned position. The torque ripple content is obviously very substantial, however it is apparent that the motor can still produce a considerable amount of average torque.

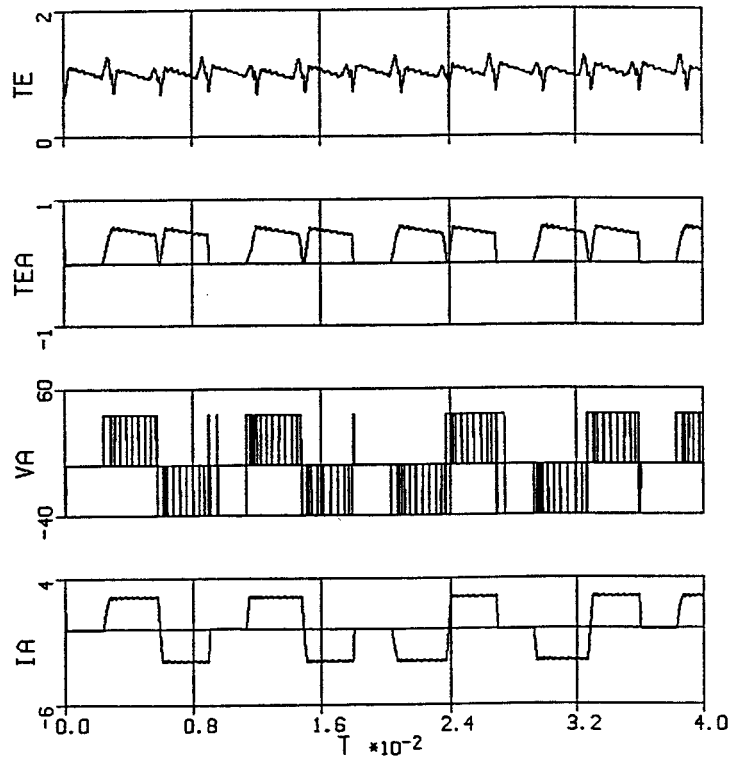

Fig. 8 Simulated Waveforms for the Prototype DSPM Motor at Low Speed.

The output power and average torque are evaluated by simulation and the capability curve of the prototype DSPM motor is shown in Fig. 10, indicating this motor can run constant power up to 2 times the base speed. The effect of the reluctance torque at high speed is clearly shown in the figure.

Table I shows the comparison of major performance indices of the prototype motor as against other motors as designed by T.J.E. Miller[17]. It can be seen that the present motor exceeds by far even the PM-BLDC motor with its high energy rare-earth PM material in terms of torque density. This can be attributed to the use of a higher flux concentration, thus higher airgap flux density made possible with the present motor design. The torque-to-inertia ratio of the DSPM motor is also very impressive as can be seen from Table I.

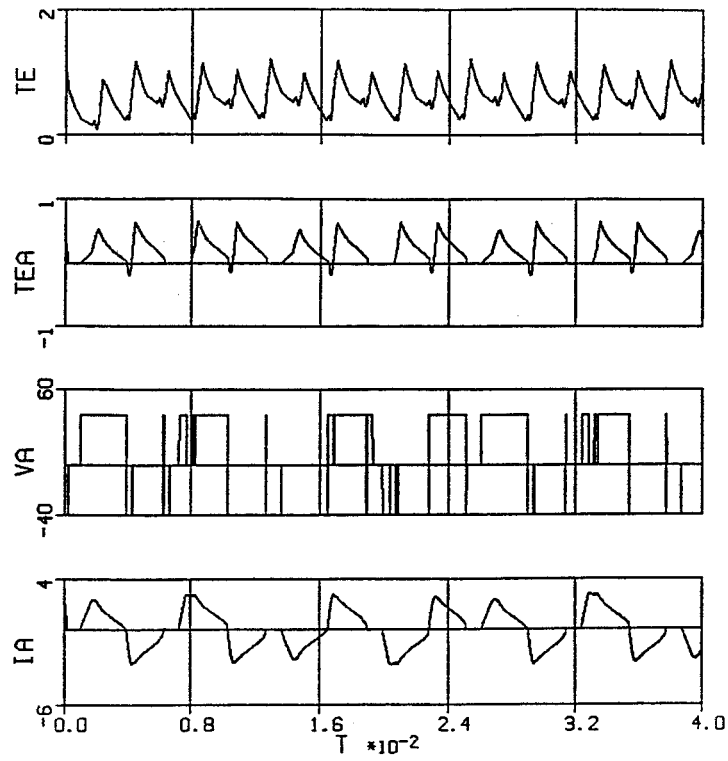

Fig. 9 Simulated Waveforms for the Prototype DSPM Motor for High Speed.

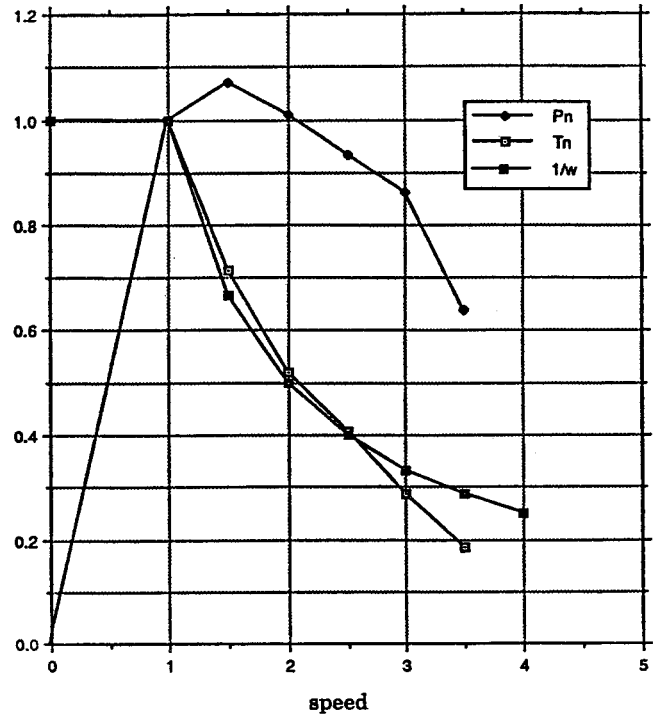

Fig. 10 Capability Curve for the Prototype DSPM Motor.

Table I Comparison of Performance for Several Different Motors of Same Rating

Parameters	PM-BLDC* Ferrite Mag.	DSPM R.E Mag	PM-Synch* R.E. Mag	IM*	SRM*	SynRM*
Phases	3	3	2	2	3	2
Poles	4	6/4	4	4	6/4	4
Stator OD(mm)	77	77.8	77.8	77.8	73.7	77.8
Stack(mm)	50	50	50	50	44.5	50
Airgap(mm)	.40	.45	.45	.20	.20	.20
Copper Wt(lbs)	0.64	0.61	0.64	0.64	0.64	0.64
Magnet Wt(lbs)	0.24	0.1	0.35	-	-	-
Total Wt(lbs)	2.64	4.23	3.81	3.39	2.71	3.45
Torque(mNm)	329	955	702	250	346	250
Torque(pu)	1.00	2.90	2.13	0.76	1.05	0.76
P_{cu-s}(watts)	14.1	13.6	13.6	13.7	14.3	13.7
$R_1(\Omega)$	2.9	0.91	1.9	1.9	2.9	1.9
$I_{s(rms)}$(A.)	1.30	2.21	1.9	1.9	1.3	1.9
Torque/Current(%)	100	170	146	52	105	52
Rotor Inertia	100	50	134	134	25	109
Torque/Inertia (%)	100	580	159	57	414	70

* Denotes Data from Ref. 20, R.E. = Rare Earth Magnets, PM-BLDC = Permanent Magnet Brushless DC (Surfact Magnets), PM-Synch = Buried Magnet PM Machine, IM - Induction Machine, SRM = Switched Reluctance Machine, SynRM = Synchronous Reluctance Machine.

4. CONCLUSION

This paper has presented a new type of doubly salient PM machine using rotating permanent magnets. The advantages of the DSPM motor are summarized as follows:

- High torque density and high efficiency;
- Simple structure and low manufacturing cost;
- Low inertia and high speed capability;
- Minimum VA ratings of the power converter.

In general, with its superior performance in torque production and with structural simplicity which is amenable to automatic manufacture, the DSPM motor drive may serve as a potential alternative to existing servo and industrial AC motor topologies, especially in small frame sizes, for variable speed drives. It is especially suitable for applications where size and weight are critical.

5. REFERENCES

[1] Lawrenson, P.J., Stephenson, J.M., Blenkinsop, P.T., Corda J. and Fulton, N.N., "Variable Speed Switched Reluctance Motors", *Proc. IEE*, pt. B, vol. 127, July 1980, pp. 253-65.

[2] Ray, W.F., Lawrenson, P.J., Davis, R.M., Stephenson, J.M. Fulton, N.N. and Blake, R.J., "High Performance Switched Reluctance Brushless Drives", *IEEE Trans. on Industry Applications*, vol. IA-22, No.4 , 1986, pp. 722-30.

[3] Stephenson, J. M., and Blake, R. J., "The Design and Performance of a Range of General - Purpose Industrial SR Drives for 1 KW to 110 KW", *Record of IEEE IAS Annual Meeting*, 1989, pp. 99-107.

[4] T.J.E. Miller and T.M. Jahns, "A Current-Controlled Switched Reluctance Drive for FHP Applications", *Proc. Conf. on Applied Motion Control (CAMC),* Minneapolis, June 1986.

[5] Miller, T.J.E. and McGilp, M., "Nonlinear Theory of the Switched Reluctance Motor for Rapid Computer-Aided Design", *IEE Proceedings,* Vol. 137, Pt. B, No. 6, November 1990, pp.337-347.

[6] J.T. Bass et al., "Simplified Electronics for Torque Control of Sensorless Switched Reluctance Motors", *IEEE Trans. on Industrial Electronics*, vol. IE-34, pp. 234.
[6] B.K. Bose et al., "Microprocessor Control of Switched Reluctance Motors", *IEEE Trans. on Industrial Applications*, vol. IA-22, 1986, pp.708-15.
[7] Richter, E., "Switched Reluctance Machines for High Performance Operation in a Harsh Environment -- A Review Paper", *International Conference on Electrical Machines*, Cambridge, Massachusetts, August 12-15, 1990.
[8] Finch, J.R. et al., "Prediction Methods for Saturated Hybrid and Variable Reluctance Motors: A Comparison", *International Conference on Electrical Machines*, Cambridge, Massachusetts, August 12-15, 1990.
[9] Mecrow, B.C. and Jack, A.G., "A New high Torque Density Permanent Magnet Machine Configuration", *International Conference on Electrical Machines*, Cambridge, Massachusetts, August 12-15, 1990.
[10] J.H. Walker,"The Theory of the Inductor Alternator", *Jounal of IEE*, vol.89,Pt.II, 1942, pp.227-241.
[11] J.T. Duane, "A Brushless DC Generator for Aircraft Use", *Trans. AIEE*, Pt.II, Nov. 1958, pp.365-372.
[12] M.J. Wright, "Advances in Automobile Battery Charging Equipment", *Direct Current*, Nov. 1965, pp.171-176.
[13] Rauch, S.E. and Johnson, L.J., "Design Principles of Flux-Switch Alternators", *A.I.E.E. Trans.* Dec. 1955, pp. 1261-68.
[14] R.L. Zimmerman, US Patent, 2,816,240, 1957.
[15] Philips, D.A., "Switched Reluctance Drives: New Aspects", *IEEE Power Electronics Specialists Conference (PESC)*, 1989, pp. 579-584.
[16] V. Torok, US Patent, 4,349,605,1982.
[17] V. Torok, US Patent, 3,995,203,1976.
[18] Lipo, T.A., Liao, Y. and Liang, F., "A New Class of Variable Reluctance Motor with Permanent Magnet Excitation", U.S. Patent Pending.
[19] Liao, Y., Liang, F. and Lipo, T.A., "A Novel Permanent Magnet Motor with Doubly Salient Structure",IAS Annual Meeting, Houston, Oct. 1992, pp. 308-314.
[20] Miller, T.J.E. et al. "Design of a Synchronous Motor Drive." *IEEE IAS Annual Meeting*, 1989, pp.122-127.

Appendix
Design Data for the Prototype DSPM Machine

Main Dimensions			
Outer Diameter (D_{OS})	77.8 mm	Inner Diameter (D_{iS})	40.0 mm
Stack Length (L_{eff})	50 mm	Air Gap Length (g)	0.45 mm
Stator Pole Arc (β_S)	30 degrees	Rotor Pole Arc (β_r)	36 degrees
Depth of Stator Poles	11.4 mm	Depth of Rotor Poles	4.9 mm
Stator Winding Details			
Wire Gauge (AWG)	20	Mean Length of Turn	152 mm
Turns/Phase	130	Parallel Circuits	1
Slot Fill	36%	Stacking Factor	0.95
Electric and Magnetic Loading			
Gap Flux Density B_g	14.55 kG	Surface Current Density A_S	351 A/inch
Current Density J	2781 A/in^2		
Motor Parameters	(Calculated)		
R_S=0.91 Ω @ 110°C	L_u = 2.7 mh	L_{com} = 4.3 mh	